SUPPLEMENTAL DATA

SUPPLEMENTAL TABLE S1
Reversible photobleaching of EYFP

From FRAP experiments similar to those shown in supplemental Fig. S4, M_f and $t_{1/2}$ were calculated for EYFP-IP_3R1 for live cells and for cells fixed in paraformaldehyde (3.5%) or methanol/acetone (1:1). Results are means ± SEM from n cells. These results demonstrate considerable recovery of EYFP fluoresecence after photobleaching on a timescale that would undermine analyses of IP_3R diffusion. Similar analyses with EGFP-IP_3R1 (supplemental Fig. S3) confirm that there is no such problem with EGFP.

	EYFP-IP_3R1 live	EYFP-IP_3R1 paraformaldehyde	EYFP-IP_3R1 methanol/acetone
M_f, %	78 ± 2	30 ± 2	24 ± 1
$t_{1/2}$, s	52 ± 3	28 ± 4	32 ± 6
n	32	22	15

SUPPLEMENTAL TABLE S2
Comparison of M_f and D for IP_3R determined in this and other studies

	D $\mu m^2/s$	M_f %	System	Reference
IP_3R1	0.26 ± 0.10	-	Hippocampal neurons	(20)
	0.010 ± 0.001	>90	Non-polarized MDCK cells	(22)
	0.004 ± 0.001	64 ± 11	Polarized MDCK cells	(22)
	~0.05	>70	RBL-2H3 cells	(11)
	0.011-0.022	~80	SH-SY5Y cells	(21)
	0.003[a]	ND	SH-SY5Y cells	(47)
	0.012[a]	ND	SH-SY5Y cells	(18)
	0.30 ± 0.029	ND	Purkinje neurons	(23)
	0.018 ± 0.001	84 ± 2	COS-7 cells	Current work
IP_3R2	0.004 ± 0.001	47 ± 4	COS-7 cells	Current work
IP_3R3	0.45 ± 0.13	ND	Hippocampal neurons	(20)
	0.031 ± 0.002	67 ± 3	CHO cells	(19)
	0.044 ± 0.003	77 ± 2	COS-7 cells	(19)
	0.28 ± 0.024	ND	Purkinje neurons	(23)
	0.016 ± 0.002	80 ± 2	COS-7 cells	Current work

[a]Determined by functional assays of local Ca^{2+} release, rather than by direct measurement of IP_3R mobility. ND, not determined.

SUPPLEMENTAL REFERENCES

49. Valentin, G., Verheggen, C., Piolot, T., Neel, H., Coppey-Moisan, M., and Bertrand, E. (2005) *Nat. Methods* **2**, 801
50. Kirber, M. T., Chen, K., and Keaney, J. F., Jr. (2007) *Nat. Methods* **4**, 767-768
51. Miyawaki, A., and Tsien, R. Y. (2000) *Methods Enzymol.* **327**, 472-500
52. McAnaney, T. B., Zeng, W., Doe, C. F., Bhanji, N., Wakelin, S., Pearson, D. S., Abbyad, P., Shi, X., Boxer, S. G., and Bagshaw, C. R. (2005) *Biochemistry* **44**, 5510-5524
53. van der Krogt, G. N., Ogink, J., Ponsioen, B., and Jalink, K. (2008) *PLoS ONE* **3**, e1916
54. Rodighiero, S., Bazzini, C., Ritter, M., Furst, J., Botta, G., Meyer, G., and Paulmichl, M. (2008) *Cell. Physiol. Biochem.* **21**, 489-498
55. Tanaka, K. A., Suzuki, K. G., Shirai, Y. M., Shibutani, S. T., Miyahara, M. S., Tsuboi, H., Yahara, M., Yoshimura, A., Mayor, S., Fujiwara, T. K., and Kusumi, A. (2010) *Nat. Methods* **7**, 865-866
56. Saffman, P. G., and Delbruck, M. (1975) *Proc. Natl. Acad. Sci. USA* **72**, 3111-3113
57. Mitra, K., Ubarretxena-Belandia, I., Taguchi, T., Warren, G., and Engelman, D. M. (2004) *Proc. Natl. Acad. Sci. USA* **101**, 4083-4088
58. Luckey, M. (2008) *Membrane structural biology*, Cambridge University Press, Cambridge

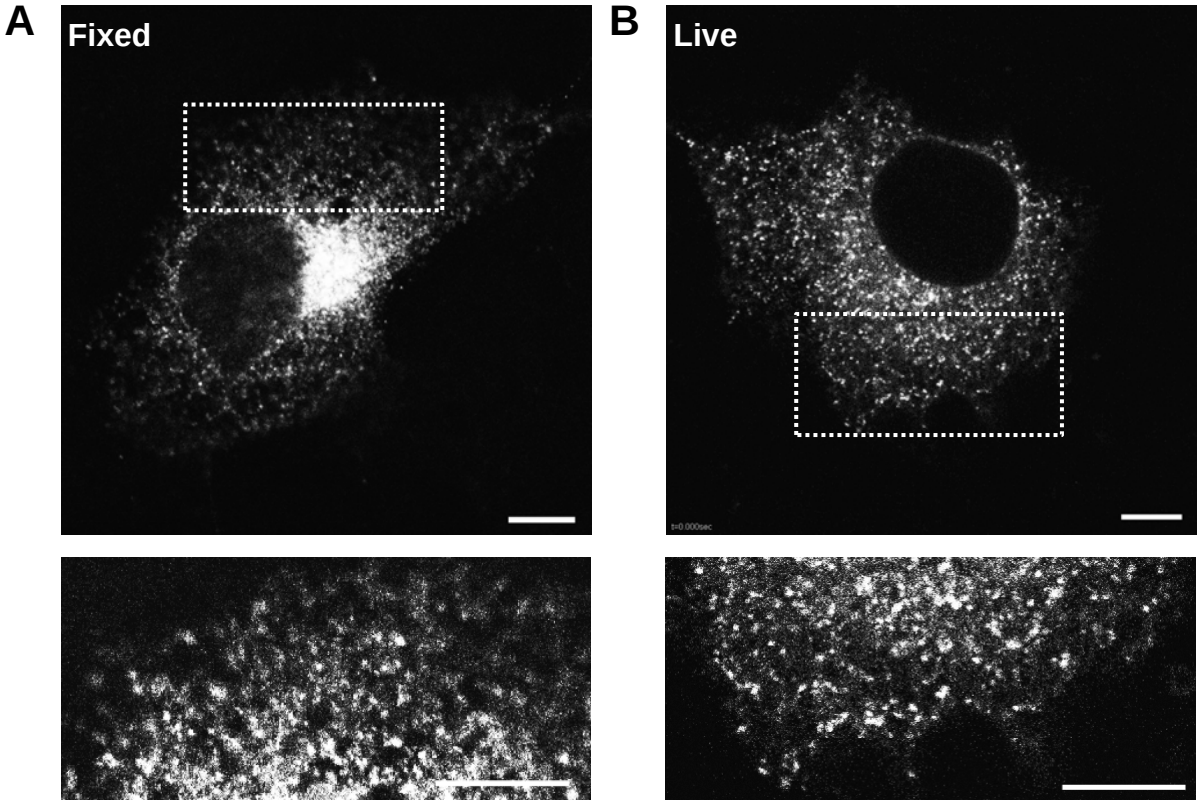

SUPPLEMENTAL FIGURE S1. **The punctate distribution of IP_3R2 is similar in live and fixed cells.** Cells transiently transfected with EGFP-IP_3R2 were imaged (*A*) after fixation with methanol/acetone (1:1, v/v) on coverslips or (*B*) live on glass-bottomed dishes. The characteristic punctate distribution of IP_3R2 is shown for both conditions (lower panels) in the enlarged images of the areas highlighted in the main panels. Scale bars = 10 μm.

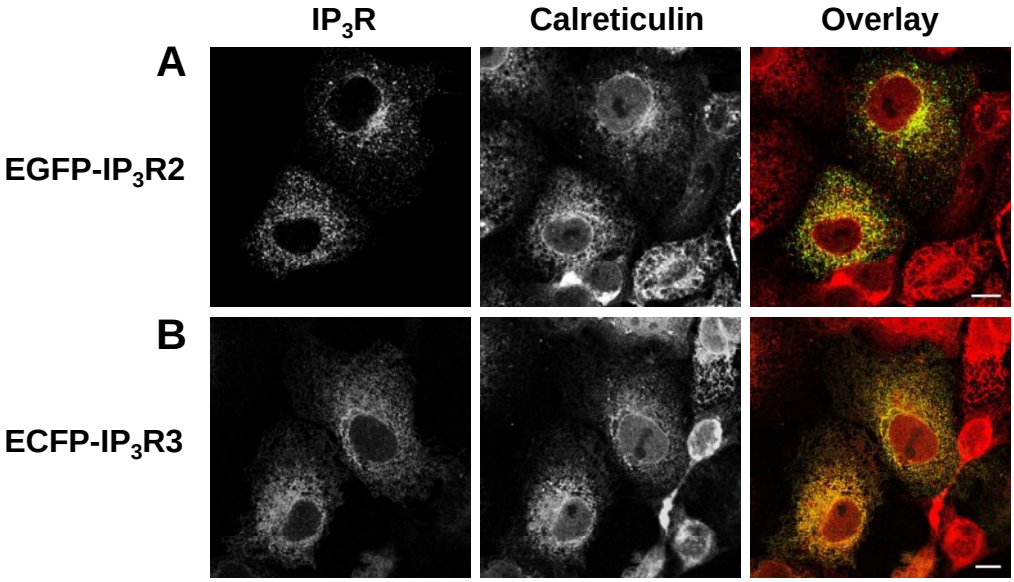

SUPPLEMENTAL FIGURE S2. **Representative fields of cells expressing IP_3R2 and IP_3R3.** Cells transfected with the indicated constructs are shown in the same format as in Fig. 1, but at lower magnification. A previous publication (28) showed a similar view for IP_3R1. Scale bars = 10 µm.

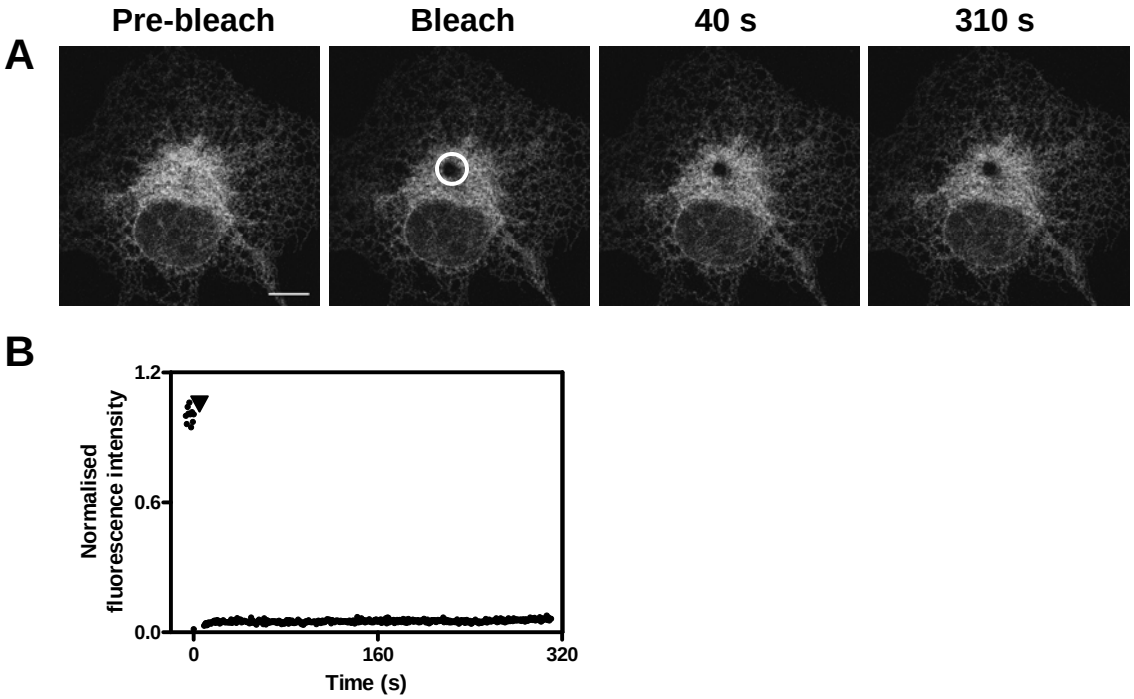

SUPPLEMENTAL FIGURE S3. **EGFP fluorescence does not recover after photobleaching of fixed cells.** *A* and *B*, COS-7 cells expressing EGFP-IP_3R1 were fixed in paraformaldehyde before FRAP analysis. *A*, Four images from a typical cell show fluorescence before bleaching, immediately afterwards, and either 40 s or 310 s after bleaching. Scale bar = 10 μm. *B*, Time course of normalized fluorescence (see Experimental Procedures) recorded from the ROI (circle in panel *A*) before and after bleaching. The arrow head shows the time of bleaching. The results, typical of recordings from 10 cells from 3 independent transfections, confirm that there is no recovery of EGFP fluorescence within the ROI after photobleaching.

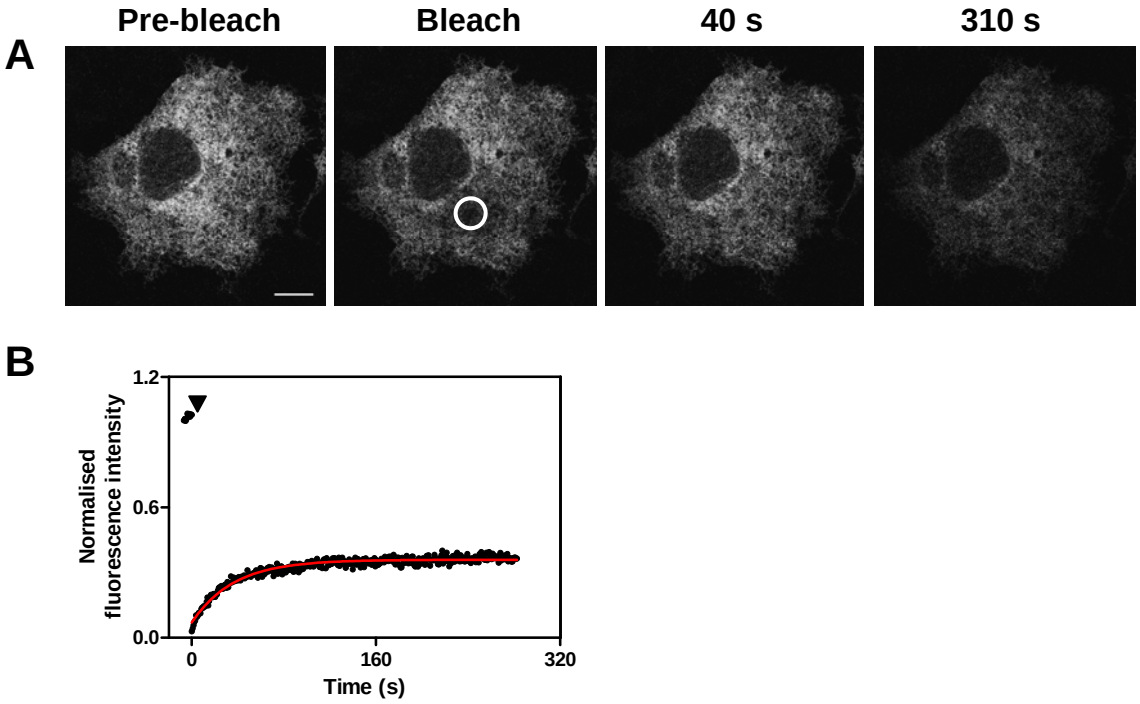

SUPPLEMENTAL FIGURE S4. **Reversible photobleaching of EYFP compromises FRAP analysis.** *A* and *B*, The experiment and presentation are as shown in supplemental Fig. S3, but with COS-7 cells transfected with EYFP-IP_3R1, rather than EGFP-IP_3R. Scale bar = 10 μm. The results demonstrate substantial recovery of EYFP within the ROI (circled in A) after photobleaching of the ROI (at the arrow head) in a cell fixed with paraformaldehyde. Results from similar experiments are summarized in supplemental Table S1. Problems with reversible bleaching of YFP (49-52) and anomalous FRET results using YFP as an acceptor have been reported, but the difficulties (35,53,54) appear not to have been widely acknowledged. Excitation of YFP at 405 or 488 nm has been reported to cause it to photoconvert to a CFP-like fluorophore that emits light detectable in the 435-485 nm region (49,50). This is unlikely to account for our observations, where EYFP was excited at 514 nm and detected at 520-600 nm. Although a recent study suggests that some membrane proteins may remain mobile after some fixation treatments (55), that cannot provide the explanation for our results because identical experiments with EGFP-IP_3R1 allowed no recovery after bleaching (supplemental Fig. S3). We avoided EYFP-tagged constructs in our FRAP analyses.

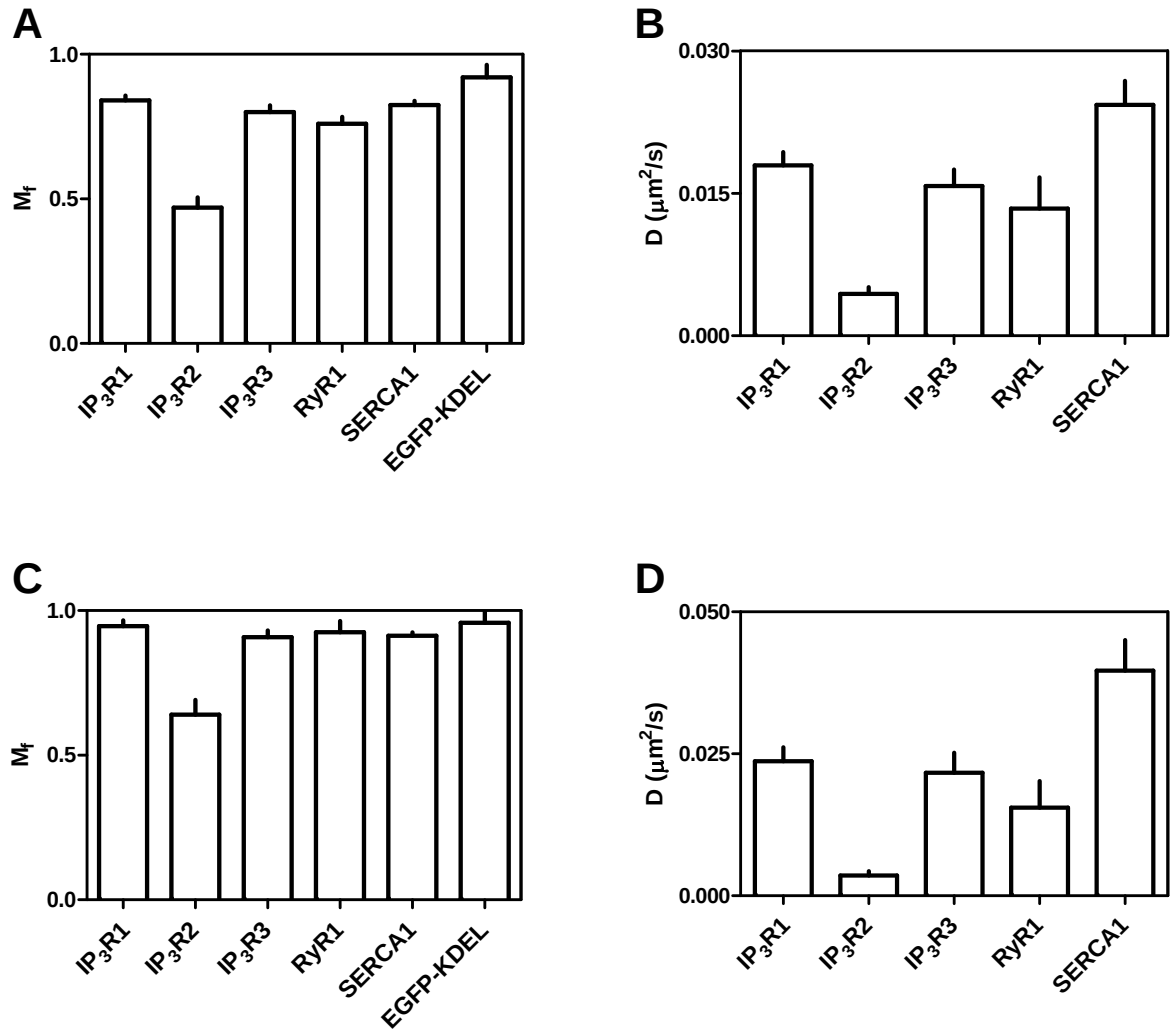

SUPPLEMENTAL FIGURE S5. **Two methods of deriving D and M_f from time courses of fluorescence recovery provide similar results.** *A-D*, From experiments similar to those shown in Fig. 3, two different methods were used to derive M_f and D from the FRAP time course for each of the six proteins examined. The very rapid diffusion of the luminal protein (EGFP-KDEL) prevented measurement of D for it. *A* and *B*, Results obtained using the single exponential analysis applied throughout this work are shown (see Experimental Procedures): $F_t = F_0 + (F_{max}–F_0)(1\text{-}e^{-kt})$, where F_t is the corrected fluorescence recorded from the ROI at time, t; F_0 and F_{max} are the fluorescence values obtained by extrapolation to immediately after the bleach and at infinite time after recovery, respectively; k is the first order rate constant for recovery. *C* and *D*, The same experimental data were also fitted to a more complex recovery curve (36,43): $F_t = F_0 + (F_{max}–F_0)t/(t+t_{½})$, where $t_{½}$ is the time for half-maximal recovery. For both curve-fitting methods, M_f and D were calculated as described in Experimental Procedures. Results are means ± SEM from 13-30 cells.

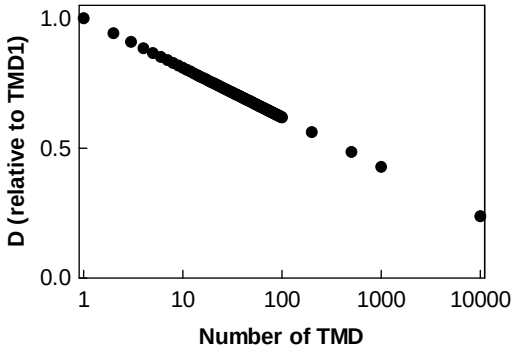

SUPPLEMENTAL FIGURE S6. **D for membrane proteins is almost independent of their size.** The diffusion coefficient (D) is related to the size of a protein (radius, r) and viscosity of the medium (η): D = kT/6πηr, where k is Boltzmann's constant and T is the absolute temperature. Because lipid bilayers are considerably more viscous than cytosol, D for an unrestrained membrane protein is much lower than for a cytosolic protein. D for a membrane-spanning protein is dominated by slow diffusion of its membrane-embedded elements. Lateral diffusion of a membrane protein is described by the Saffman-Delbruck equation (56):

$$\mathrm{D} = \frac{\mathrm{kT}}{4\pi\eta_\mathrm{m}\,\mathrm{h}}\left(ln\frac{\eta_\mathrm{m}\,\mathrm{h}}{\eta_\mathrm{w}\,\mathrm{r}} - 0.5772\right)$$

where, η_m and η_w are the viscosities of the membrane and surrounding aqueous environment, respectively; h is the thickness of the membrane; r is the radius of the membrane-embedded protein. η_m ~100 mPa·s and η_w ~1 mPa·s (56). For two membrane proteins with different radii (r_1 and r_2), but embedded in the same membrane:

$$\frac{\mathrm{D}_1}{\mathrm{D}_2} = \frac{ln\frac{\eta_\mathrm{m}}{\eta_\mathrm{w}} + ln\frac{\mathrm{h}}{\mathrm{r}_1} - 0.5772}{ln\frac{\eta_\mathrm{m}}{\eta_\mathrm{w}} + ln\frac{\mathrm{h}}{\mathrm{r}_2} - 0.5772} \approx \frac{4.028 + ln\frac{\mathrm{h}}{\mathrm{r}_1}}{4.028 + ln\frac{\mathrm{h}}{\mathrm{r}_2}}$$

The ER membrane is ~3.75 nm thick (57) and a typical membrane-spanning α-helix has a radius of ~0.5 nm (58). Assuming close-packing of *N* α-helices of a membrane-spanning protein, the radius of the protein (r, in nm) is approximately: r = ~0.5 nm√N. This provides the simplified relationship, from which it is clear that D is scarcely affected by the size of the protein:

$$\frac{\mathrm{D}_1}{\mathrm{D}_2} \approx \frac{4.028 + ln\frac{3.75}{0.5\sqrt{\mathrm{N}_1}}}{4.028 + ln\frac{3.75}{0.5\sqrt{\mathrm{N}_2}}} = \frac{6.043 - ln\sqrt{\mathrm{N}_1}}{6.043 - ln\sqrt{\mathrm{N}_2}}$$

The graph shows the relationship, as defined above, between the number of transmembrane domains (TMD) and the predicted D of a membrane-spanning protein. Results are expressed relative to D for a protein with a single TMD. The important point is that for typical membrane-spanning proteins, D depends only weakly on their size.

D averaged for IP_3R1 and IP_3R3, each with 24 TMD, is 0.017 $\mu m^2/s$; and for SERCA1, with 10 TMD, it is 0.024 $\mu m^2/s$. The difference in D for the two proteins (D_1/D_2 = 1.41), which is similar to that reported for SERCA2a and IP_3R1 (D_1/D_2 = 1.30-1.81) (20,23), is larger than predicted for two proteins with 10 and 24 TMD (D_1/D_2 = 1.10) and more consistent with proteins with 10 and ~170 TMD. While there is some danger of over-interpreting FRAP data, the disparity leaves open the possibility that either the mobility of IP_3R is more restricted than that of SERCA, or that D for IP_3R1 and IP_3R3 may report the diffusion of small clusters of IP_3R (~7 tetrameric subunits) rather than single IP_3R. D for IP_3R2 (0.004 $\mu m^2/s$) is much lower than the average for IP_3R1 and IP_3R3 (0.017 $\mu m^2/s$) (Table 1). If the difference were due only to the larger size of IP_3R2 clusters, the ratio of the diffusion coefficients (D_1/D_2 = 4.25) predicts that IP_3R2 clusters must include at least 900 IP_3R. Given the density of IP_3R2 puncta in each cell (Fig. 1, *B* and *C* and Fig. 4*E*) and the observation that typical cells probably express no more than 10^5 IP_3R/cell (48), it is implausible to suggest that each punctum includes >900 IP_3R2. We conclude, therefore, that clustering of IP_3R2 is not the direct cause of their reduced motility.

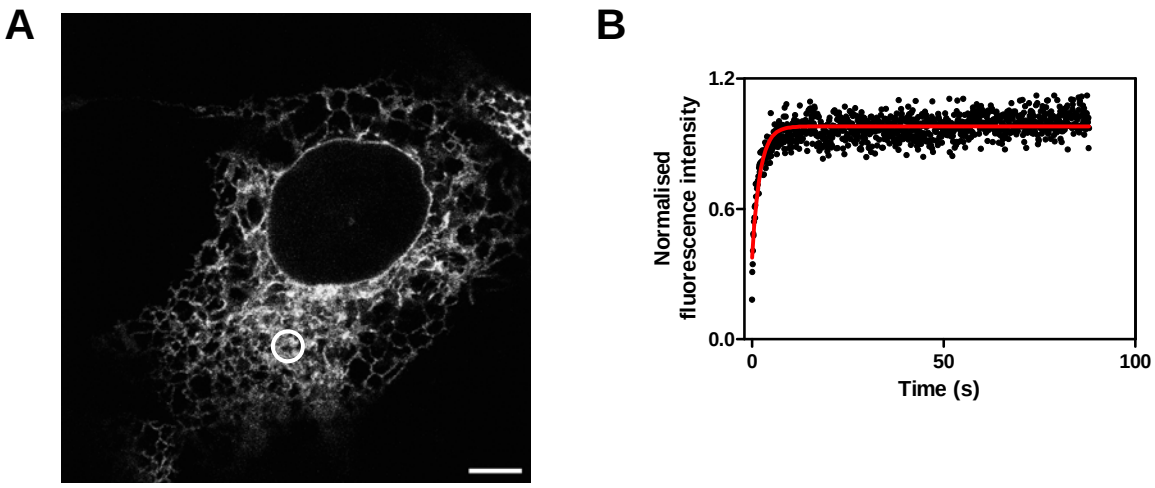

SUPPLEMENTAL FIGURE S7. **M_f for a luminal ER protein, EGFP-KDEL.** *A*, COS-7 cell expressing EGFP-KDEL. Scale bar = 10 μm. *B*, Time-course of normalized fluorescence recorded from the ROI after bleaching. The results are typical of recordings from 17 cells.